Optical Fiber Technology 52 (2019) 101996

Contents lists available at ScienceDirect

Optical Fiber Technology

journal homepage: www.elsevier.com/locate/yofte

Holmium oxide thin film as a saturable absorber for generating Q-switched and mode-locked erbium-doped fiber lasers

Ahmed Shakir Al-Hiti[a], M.F.A. Rahman[a,b], S.W. Harun[a,*], P. Yupapin[c,d], M. Yasin[e,*]

[a] Department of Electrical Engineering, Faculty of Engineering, University of Malaya, Kuala Lumpur 50630, Malaysia
[b] Fakulti Teknologi Kejuruteraan Elektrik & Elektronik, Universiti Teknikal Malaysia Melaka, 76100 Hang Tuah Jaya, Melaka, Malaysia
[c] Computational Optics Research Group, Advanced Institute of Materials Science, Ton Duc Thang University, Ho Chi Minh City, Viet Nam
[d] Faculty of Applied Sciences, Ton Duc Thang University, Ho Chi Minh City, Viet Nam
[e] Department of Physics, Faculty of Science and Technology, Airlangga University, Surabaya 60115 Indonesia

ARTICLE INFO

Keywords:
Q-switched
Mode-locked
ERBIUM-doped fiber laser
Ho_2O_3
Saturable absorber

ABSTRACT

We demonstrated a new type of transition metal oxide (TMO) material, Holmium oxide (Ho_2O_3) polymer film SA for compact passively Q-switched and mode-locked erbium-doped fiber laser (EDFL) generations. The film SA has a thickness of ~40 μm and modulation depth of ~45%. It was fabricated by embedding Ho_2O_3 nanoparticles into PVA polymer solution. The Q-switched laser operated stably at a center wavelength of 1563 nm within a pump power range of 45–97 mW. The maximum Q-switching pulse repetition rate and the narrowest attainable pulse width were 115.8 kHz and 0.64 μs, respectively; while, the maximum pulse energy was obtained as 129.36 nJ. On the other hand, the mode-locked EDFL emerged stably within a pump power range of 62–180 mW at a center wavelength of 1565.4 nm. The repetition rate was 17.1 MHz, while the pulse width was 650 fs. Additionally, the maximum output power was measured as 9.01 mW; while, the corresponding maximum pulse energy was obtained as 0.524 nJ. This Ho_2O_3 film SA offers simplicity and reliability in the design of compact and portable fiber pulsed laser generators particularly in the 1.55-μm regime.

1. Introduction

Passively pulsed fiber lasers have received tremendous research attention in recent years owing to their potential applications in biomedicine, metrology, optical sensing and optical communications [1,2], to name a few. Pulsed fiber lasers can be accomplished using two common techniques; Q-switching and mode-locking. Q-switched lasers generally generate relatively longer pulse widths, in the range of nanoseconds to picoseconds; while, the mode-locked lasers generate a pulse width in the range of femtoseconds to picoseconds. These two techniques can be realized either through active or passive approaches. The passive procedure has gained growing interests in the past few years essentially due to its simplicity, flexibility, compactness and low cost of fabrication. Unlike the active procedure which uses quite bulky and complex electronics such as acousto-optic and electro-optic modulator for the pulse triggering mechanism, the passive procedure can be accomplished by incorporating a cheap and simple saturable absorber (SA) in the cavity.

In the early years, semiconductor saturable absorber mirror (SESAM) [3,4] and carbon nanotubes (CNT) [5,6] have been widely used for pulsed fiber laser generations. However, SESAM is quite costly, has narrow operating bandwidth and quite complex in fabrication [4]. Although, CNT is quite cheap and simple in fabrication; however, their operating wavelength relies very much on the diameter of the nanotubes [5], and thus has limited its potential uses. In recent years, various two-dimensional (2D) materials SA including graphene, transition metal dichalcogenides (TMD [7,8]; MoS_2, $MoSe_2$, WSe_2, WS_2, etc.), topological insulator (TI [9–11]; Bi_2Te_3, Bi_2Se_3, Sb_2Te_3, etc.) and black phosphorus (BP) [12,13] have been demonstrated in the literature as passive pulsed modulators. Although these 2D SAs are quite successful, they also have certain drawbacks. The graphene SA, for instance, has low absorption efficiency of 2.3% at 1550 nm [14]. The TMD materials have a quite low modulation depth and have large direct band-gap which are not so effective to be used for longer wavelengths despite having low impurity and uniformity [15,16]. The TI materials are quite difficult to fabricate because of the existence of two different elements. The BP, on the other hand, is hydrophilic material and its reaction with high humidity environment would affect its overall performance [17].

Besides these 2D materials, a few of material oxides such as titanium dioxide (TiO_2) [18], nickel oxide (NiO) [19] and holmium oxide

* Corresponding authors.
E-mail addresses: swharun@um.edu.my (S.W. Harun), yasin@fst.unair.ac.id (M. Yasin).

https://doi.org/10.1016/j.yofte.2019.101996
Received 29 June 2019; Received in revised form 10 August 2019; Accepted 15 August 2019

(Ho_2O_3) [20] have also gained interests in the recent years for pulse modulators. These material SAs (commonly in film structure), are quite cheap, compact in nature, easy to prepare and handle; besides, shows a good self-starting and high compatibility with fiber lasers system. In the previous report, Ho_2O_3 was demonstrated able to facilitate a reliable performance of Q-switched pulsed laser in the 2-μm region [20]. The existence of oxides element in the Ho_2O_3 as well other oxides materials yield sufficient saturable absorption at certain regions. Furthermore, the metallic oxide particularly holmium oxide material has a considerably high modulation depth of around 45% which is useful in the pulsed laser generation. The material is chemically stable and can be easily dispersed into the PVA (host material) through solutions mixing and stirring.

In this regard, we demonstrate a compact and simple mode-locked Erbium-doped fiber laser by using a ~40 μm thick Ho_2O_3 polymer film SA. The film SA was fabricated by homogenously embedding Ho_2O_3 nanoparticles in the polyvinyl alcohol (PVA) solution. The Q-switched EDFL repetition rate can be tuned within a frequency range of 104.8–115.8 kHz at a corresponding pump power range of 45–97 mW. On the other hand, the mode-locked EDFL was stably attained by incorporating the Ho_2O_3 film SA together with a 3 m single mode fiber (SMF 28) in the cavity. The mode-locked laser generated a stable repetition rate of 17.1 MHz and a pulse width as narrow as 650 fs within a pump power range of 62–180 mW.

2. Ho_2O_3 PVA film SA fabrication and characteristics

The Ho_2O_3 PVA film was fabricated by homogenously mixing Ho_2O_3 nano-powder (obtained from Sigma-Aldrich (M)) into PVA solution. The Ho_2O_3 powder is stated by the manufacturer to have an average particle size of < 100 nm and a purity of 99%. The whole fabrication processes of the Ho_2O_3 film SA is provided in Fig. 1. Initially, 1 g of PVA was dissolved into 100 ml of distilled (DI) water. The PVA solution was consistently stirred using a magnetic stirrer for ~4 h at a constant speed of 200 rpm. Next, 1 ml of the PVA solution was transferred into a graduated cylinder. Later, 5 mg of the Ho_2O_3 nano-powder was gently poured into the prepared 1 ml PVA solution. The PVA solution which contained the Ho_2O_3 powder was then stirred at a constant speed using a magnetic stirrer for 3 h. The homogenously dispersed Ho_2O_3 PVA solution was then transferred into a clean glass petri dish. The solution was left to dry and evaporate at room temperature for 96 h, to form a semi-transparent white colored Ho_2O_3 polymer film. The Ho_2O_3 PVA film had a thickness of ~40 μm. A piece of the film SA, within the size of ~1 mm × 1 mm was gently attached on a clean FC/PC fiber ferrule with the help of index matching gel (as shown in the image in Fig. 1).

The preparation methodology of the holmium oxide film was repeated and tested for two times. The obtained pulsed laser performances using these two prepared films were quite similar. The holmium film oxide in this work was prepared at different stirring period and at different weight ratio as compared to the previous report [20]. In our case, the best pulsed laser performance was obtained by using 5 mg of holmium oxide nanopowder with 1 ml PVA solution stirred together at approximately 3 h in a controlled lab environment. The use of a correct weight of holmium oxide with a suitable stirring period will determine a good SA distribution in the host material.

The image of the fabricated film SA under a scanning electron microscope (SEM) is given in Fig. 2(a). As can be seen, the Ho_2O_3 nanoparticles were fully dispersed into the PVA film. Fig. 2(b) shows the power intensity dependent absorption profile of the Ho_2O_3 film SA which is measured by using the common balanced synchronous twin-detector approach [21,22]. As shown in the figure, the experimental data are nicely fitted with the nonlinear absorption model; $\alpha(I) = \alpha_s/(1 + I/I_{sat}) + \alpha_{ns}$, where $\alpha(I)$ is the absorption coefficient, α_s is the modulation depth, I is the input intensity, I_{sat} is the saturation intensity, and α_{ns} is the non-saturation loss. Based on the plotted absorption curve, the modulation depth of the Ho_2O_3 film SA is obtained as 45%; while, the saturation intensity and the non-saturation loss are measured as 140 MW/cm^2 and 40.2%, respectively. The modulation depth of the WO_3 is relatively higher than certain of the 2D materials [9,23]; MoS_2 (2.15%), $MoSe_2$ (6.73%), WS_2 (2.53%), WSe_2 (3.02%) and Bi_2Se_3(4.3%). Fig. 2(c) provides the energy dispersive x-ray spectroscopy (EDX) profile of the Ho_2O_3 film SA. As shown in the figure, the film SA is significantly dominated by carbon (C) with a weight percentage of 50.16%, followed by holmium (Ho) and oxygen (O), with corresponding weight percentages of 32.86% and 16.99%, respectively. The presence of these elements is due to the Ho_2O_3 and PVA which made up the composite film.

3. Pulsed laser cavity configuration

The experimental set-up of the Ho_2O_3 film SA based Q-switched EDFL is given in Fig. 3(a). The laser utilizes 2 m long erbium-doped fiber (EDF) as a gain medium. The EDF is stated by the manufacturer to have a core diameter of 4 μm, a numerical aperture of 0.16, erbium ion absorption of 23 dB/m at 980 nm and a group velocity dispersion (GVD) of 27.6 ps^{2}km^{-1}. The EDF gain medium is pumped by a 980 nm laser diode through a 980/1550 wavelength division multiplexer (WDM). The laser is then propagated into an optical isolator (ISO) which is used to prevent back reflections and to preserve unidirectional laser beam propagation in the cavity. Next, the laser is directed into a 3 dB coupler which splits the output laser into 50–50 separations, where half of the laser output is diverted out for related laser performance investigations. The remaining half of the output is circulated back inside the cavity through the Ho_2O_3 PVA film SA and the 1550 nm port of the WDM. The Ho_2O_3 film SA is incorporated into the cavity to modulate intracavity loss and thus, converts continuous wave (CW) laser into pulsed lasers at a specific range of pump power. The SA is held firmly between two fiber connectors with the assistance of index matching gel and a fiber adapter. Another 3 dB output coupler is incorporated after the first 3 dB coupler output port, to further divides the output laser into 50–50 separations for simultaneous and real-time data measurements at two different ports.

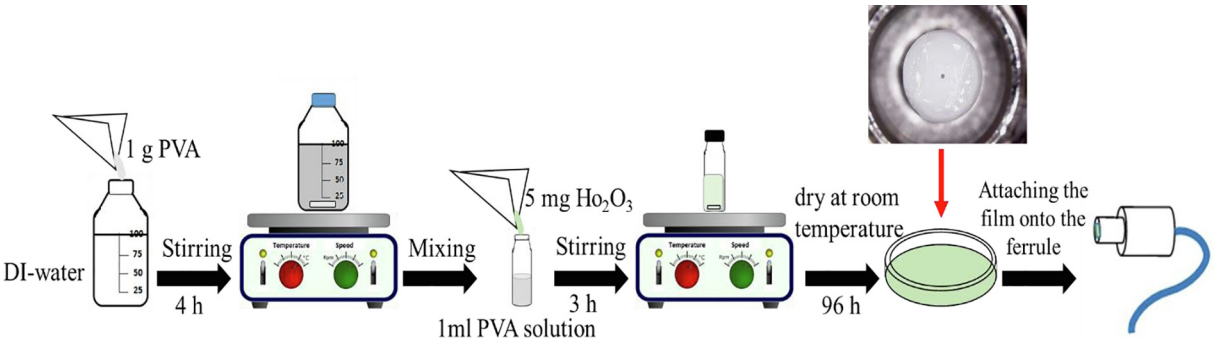

Fig. 1. The fabrication processes of the Ho_2O_3 PVA thin film.

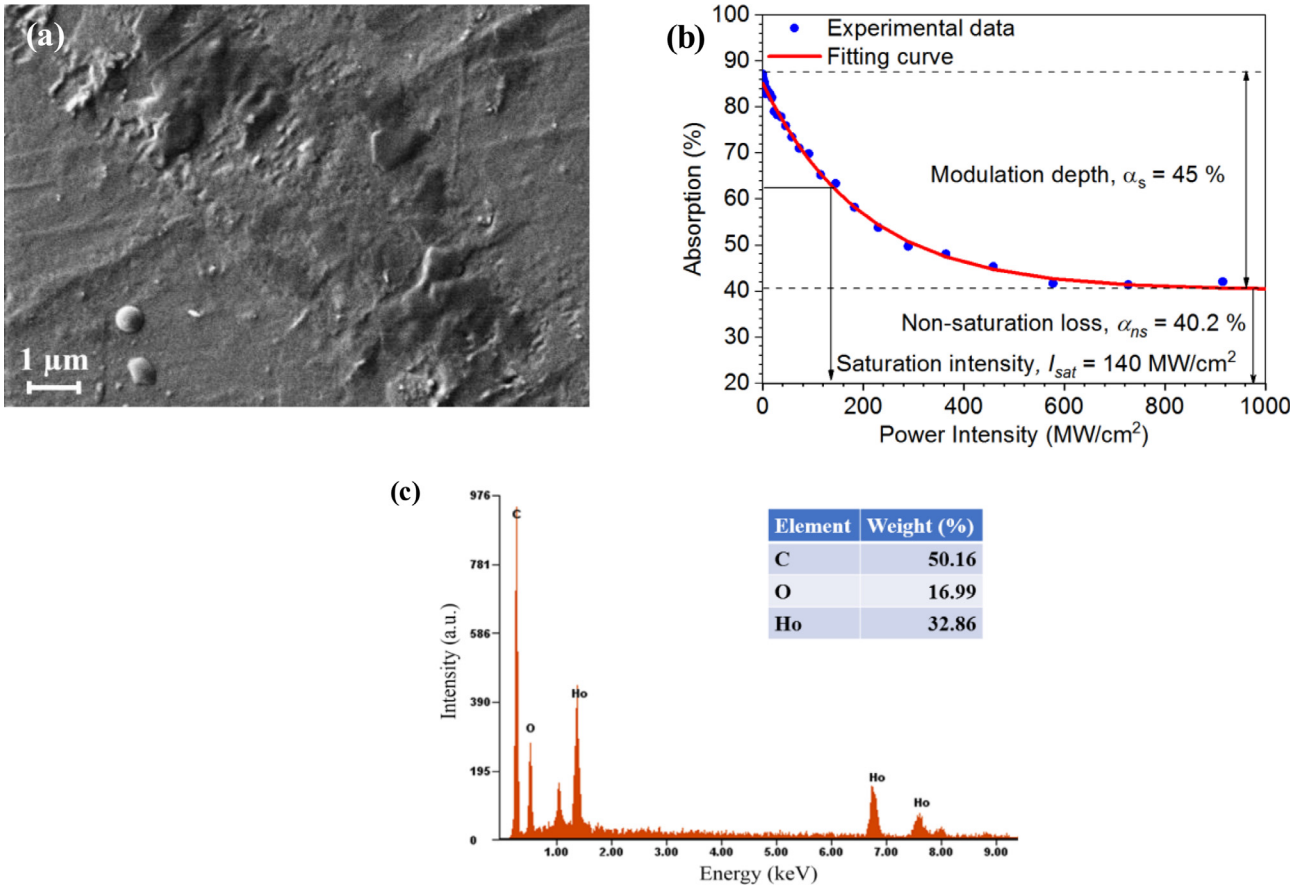

Fig. 2. Ho_2O_3 PVA film SA characteristics; (a) SEM image, (b) EDX profile, and (c) modulation depth.

The output laser was analyzed by using a digital oscilloscope (OSC), a radio frequency spectrum analyzer (RFSA), an optical spectrum analyzer (OSA) with a resolution of 0.07 nm, an autocorrelator (AC) and a power meter. The rest of the cavity was formed by single-mode fiber (SMF-28). The WDM and the SMF used in this set-up has a GVD of -48.7 and -21.7 ps^2/km, respectively. The total cavity length used for the mode-locked operation is 11.7 m; while, the total net dispersion is calculated as -0.17 ps^2 (anomalous).

The proposed mode-locked EDFL cavity as shown in Fig. 3(b) is similar as the Q-switched EDFL cavity design (Fig. 3(a)), except for several optical connections as follow. As shown in the figure, a 95/5 coupler is used instead of a 3 dB coupler for the mode-locked operation. This is to provide more output laser (95%) circulating inside the cavity; while diverts out only 5% of the output laser for various optical

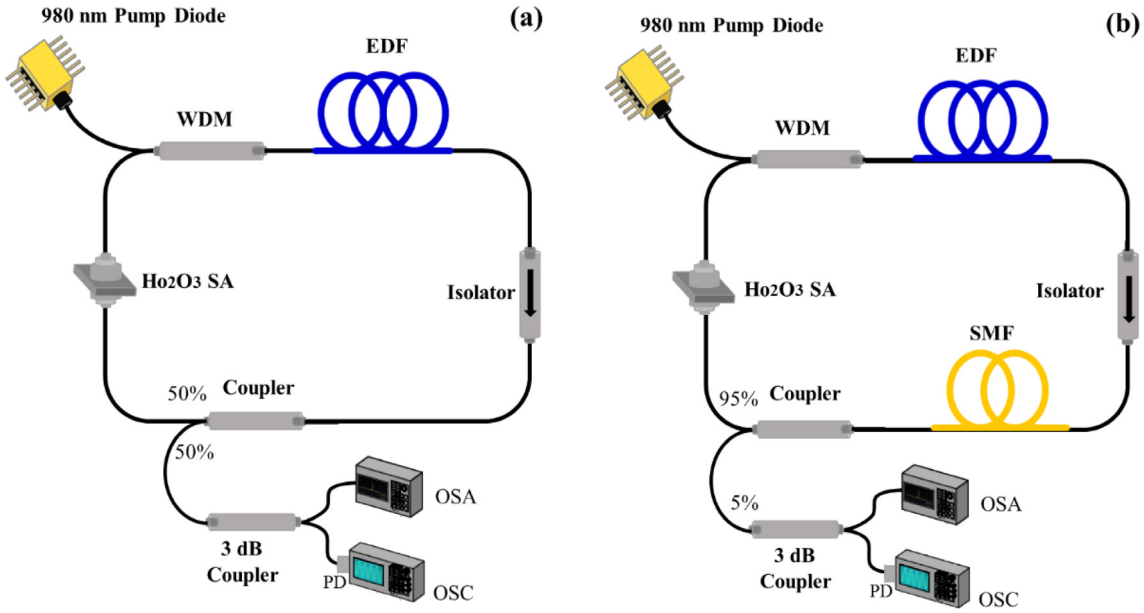

Fig. 3. Experimental setup of the EDFL pulsed laser (a) Q-switching, and (b) mode-locking.

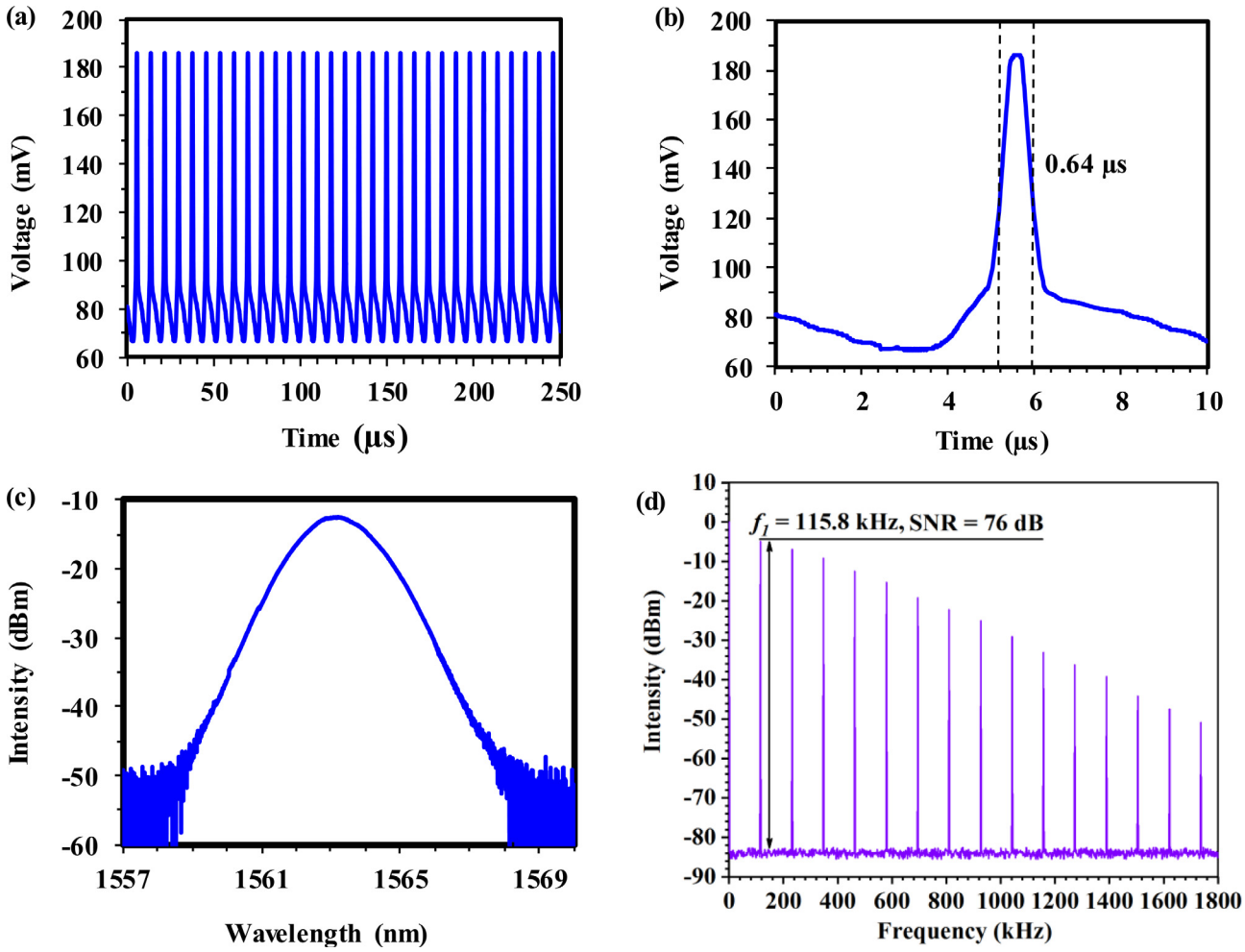

Fig. 4. Q-switched EDFL characteristics at 97 mW pump power; (a) pulses train, (b) single envelope pulse, and (c) optical spectrum.

measurements. In addition to that, 3 m long of SMF-28 is also added between the isolator and the 95/5 coupler. This is to balanced-up the intracavity dispersion and nonlinearity in the cavity so that a stable soliton mode-locked EDFL can be generated.

4. Results and discussion

The EDFL has a Q-switching repetition rate of 104.8 kHz at a Q-switching threshold pump power of 45 mW. Fig. 4 demonstrates the Q-switched EDFL characteristics at the maximum frequency 115.8. The Q-switched pulses train recorded by the OSC in the period of 250 μs is illustrated in Fig. 4(a) illustrates. As shown in the figure, the pulses train is quite stable; verified by identically similar pulse amplitudes and the pulse periods. A single pulse envelope as provided in Fig. 4(b), shows that the pulse width (measured at the full width half maximum, (FWHM)) is ~0.64 μs. The optical spectrum of the output laser as provided in Fig. 4(c) illustrates the Q-switched EDFL with a center wavelength of 1563 nm and power intensity of 12.78 dBm. The stability of the Q-switched EDFL was further investigated by the RFSA trace. The presence of many RF harmonics as depicted in Fig. 4(d) as well as a fundamental frequency, f_1 (115.8 kHz) with a considerably high signal to noise ratio (SNR) of 76 dB, verifies that the Q-switched laser is stable. The performance of the Q-switched EDFL at different pump powers is presented in Fig. 5. Fig. 5(a) shows the pulse repetition rate and pulse width performances as a function of pump power, observed within a range of 45–97 mW. As shown the repetition rate increases almost linearly from 104.8 kHz to 115.8 kHz; while, the pulse width shortens from 2.13 μs to the narrowest of 0.64 μs, in correspondence to the increase of pump power. Additionally, Fig. 5(b) shows the output power and the pulse energy which are plotted against the pump power. As illustrated, both components react linearly against the increasing pump power. The maximum output power and the maximum pulse energy are 14.98 mW and 129.36 nJ, respectively, and both are obtained at the maximum pump power of 97 mW.

The mode-locked EDFL with a repetition rate of 17.1 MHz emerged stably at a pump power range of 62–180 mW. Beyond 180 mW of pump power, the mode-locked laser became unstable and collapsed into CW laser. Fig. 6 demonstrates the mode-locked EDFL typical characteristics and performances. As shown in Fig. 6(a) the output spectrum is operated in the soliton regime with Kelly sidebands. The laser is operated in the anomalous dispersion region, while the emergence of Kelly sidebands on the left and right of the output spectrum, is attributed to a periodic disturbance of soliton pulse in the laser cavity. These considerably strong Kelly sidebands suggest that the obtained pulse frequency is considerably close to the maximum attainable value. The output laser is seen centered at the 1565.4 nm wavelength with a 3 dB spectral bandwidth of ~4.02 nm (~492.7 GHz). Fig. 6(b) shows the RFSA trace of the laser measured at a resolution bandwidth (RBW) of 100 kHz. As illustrated, there are many RF harmonics presence in the 1000 MHz frequency span, which essentially indicates that the pulse width is considerably narrow. Furthermore, the f_1 (17.1 MHz) also is seen to has a considerably high SNR of 75 dB, which further confirms the stability of the generated mode-locked pulse. The pulsed laser also is verified to be operated in the mode-locked regime, since the time taken by the light to complete a single round trip corresponds nicely to the obtained mode-locked frequency of 17.1 MHz. Additionally, the

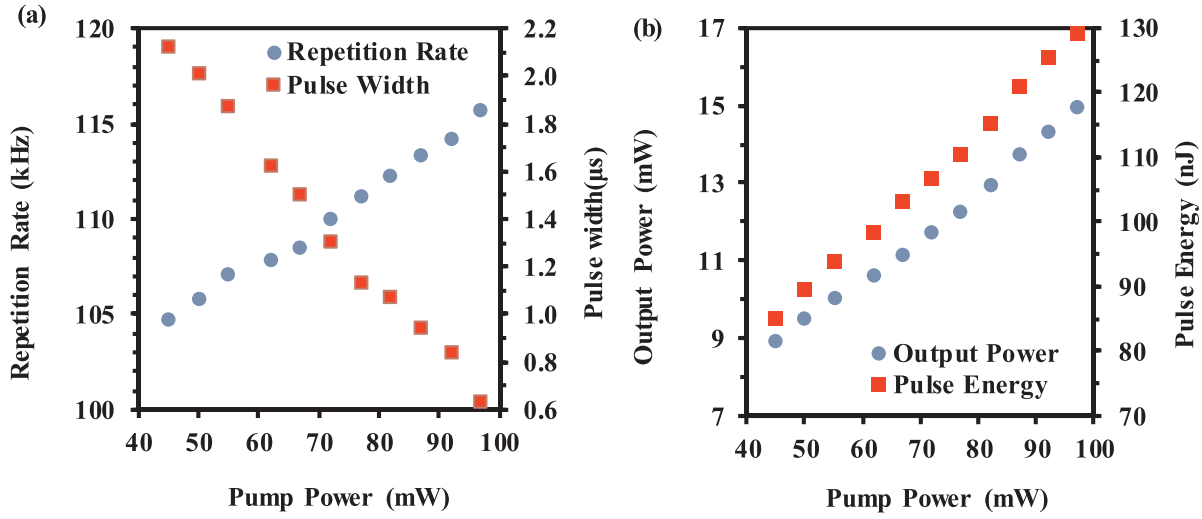

Fig. 5. Q-switched EDFL performances at different pump powers; (a) repetition rate and pulse width (b) output power and pulse energy.

autocorrelator trace of the mode-locked pulse together with its corresponding sech^2 curve fitting outline is shown in Fig. 6(c). The pulse width is measured to be 650 fs which is relatively narrow as compared to few other SAs [24–26]. The time-bandwidth product (TBP) of the laser is calculated as 0.32 and is slightly larger than 0.315 for a sech^2 shape. This indicates that the pulse is weakly chirped. Fig. 6(d) shows the output power and the pulse energy that react in an increasing manner towards the increasing pump power (62–180 mW). The maximum output power is measured as 9.01 mW; while, the highest pulse energy is calculated as 0.524 nJ.

The mode-locking phenomena can always be seen right from the mode-locking threshold pump power of 62 mW to the maximum available pump power of 180 mW. This indicates that the proposed film SA has an optical damage threshold which is greater than the maximum operating pump power of 180 mW. The experimental procedure was further repeated without incorporating the SA film inside the cavity. As

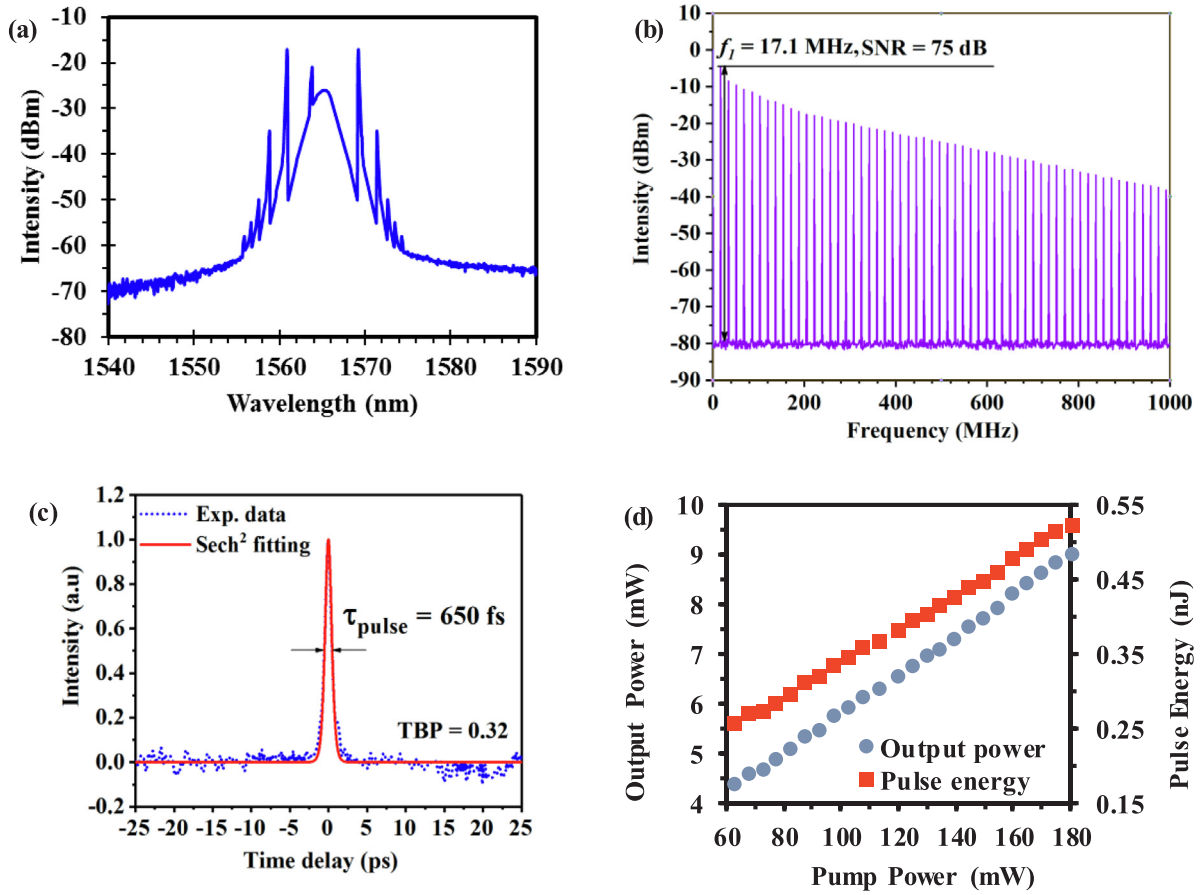

Fig. 6. Mode-locked EDFL characteristics and performances (a) optical spectrum, (b) RF spectrum, (c) autocorrelation trace and, (d) output power and pulse energy at different input pump powers.

Table 1
Various SAs characteristics and pulsed laser performances in the 1.55 μm region.

SA Material	Modulation Depth	Saturation Intensity	Central Wavelength	Rep. rate	Pulse Width	Ref.
MoS_2film)	4.3%	34 MW/cm^2.	69.5 nm	12.09 MHz	710 fs	[27]
BP	18.55%	10.74 MW/cm^2.	71.45 nm	5.96 MHz	946 fs	[28]
BPQDs	36%	3.3 GW/cm^2.	67.5 nm	15.22 MHz	1.08 ps	[29]
WS_2.	15.1%	157.6 MW/cm^2.	68.3 nm	487 kHz	1.49 ps	[30]
TiS_2.	%	9.91 MW/cm^2.	69.5 nm	5.34 MHz	1.04 ps	[31]
$PtSe_2$.	11%-4.90%	0.34 - 1.23 GW/cm^2.	63 nm	23.3 MHz	1.02 ps	[32]
FIrpic	12.8%	5.5 MW/cm^2.	62.57 nm	3.43 MHz	120 ns	[33]
Lu_2O_3 (film)	10%	100 MW/cm^2.	64 nm	0.97 MHz	2.12 ps	[34]
MgO (film)	32.4%	16 MW/cm^2.	69.1 nm	3.5 MHz	5.6 ps	[35]
V_2O_3(film)	7%	71 MW/cm^2.	59.25 nm	1 MHz	3.14 ps	[36]
NiO (film)	39%	0.04 MW/cm^2.	61.8 nm	0.96 MHz	950 fs	[37]
Sb (film)	23%	15 MW/cm^2	1559 nm	0.99 MHz	3.53 ps	[24]
Ho_2O_3 (film)	45%	140 MW/cm^2.	65.4 nm	17.1 MHz	650 fs	This work

expected, no pulsed laser could be seen, as the pump power elevated to the maximum available value. These results validate the function of the Ho_2O_3 film SA in facilitating stable Q-switched and mode-locked EDFL operations.

Table 1 shows different SAs (including certain film SAs) performances in comparison with the SA (Ho_2O_3 film) used in this work for generating mode-locked fiber lasers particularly in the ~1.55 μm wavelength region. As shown, the obtained modulation depth, saturation intensity, repetition rate and pulse width (based on the holmium oxide film) are comparable with the other SAs reported in the literature.

5. Conclusion

In this paper, we presented the first demonstration of passively Q-switched and mode-locked EDFLs by using a piece of ~40 μm thick Ho_2O_3 PVA film SA. The film SA has a modulation depth of 45% and a saturation intensity of 140 MW/cm^2. The Q-switched EDFL operated at a centre wavelength of 1563 nm. The pulse frequency and the pulse width were tunable within the range of 104.8–115.8 kHz and 2.13–0.64 μs, respectively; at a pump power range of 45–97 mW. Additionally, the maximum output power and the maximum pulse energy were obtained as 14.98 mW and 129.36 nJ, respectively. On the other hand, the soliton mode-locked EDFL emerged stably at a center wavelength of 1565.4 nm. The repetition rate and the pulse width were measured as 17.1 MHz and 650 fs, and always can be seen within a pump power range of 62–180 mW. The maximum output power, as well as the maximum pulse energy, were measured as 9.01 mW and 0.524 nJ, respectively.

Acknowledgement

This work is financially supported by Airlangga University - Mandate Research Grant (2019) and the University of Malaya (GPF005A-2018).

Appendix A. Supplementary data

Supplementary data to this article can be found online at https://doi.org/10.1016/j.yofte.2019.101996.

References

[1] U. Keller, Recent developments in compact ultrafast lasers, Nat. Photonics 424 (2003) 831–838.
[2] E. Martin, I.H. Fermann, Ultrafast fiber laser technology, IEEE J. Selected Top. Quant. Electron. 15 (1) (2009) 191–206.
[3] M. Wang, et al., Passively Q-switched Er-doped fiber laser using a semiconductor saturable absorber mirror, Optik-Int. J. Light Electron Optics 125 (9) (2014) 2154–2156.
[4] U. Keller, et al., Semiconductor saturable absorber mirrors (SESAM's) for femtosecond to nanosecond pulse generation in solid-state lasers, IEEE J. Sel. Top. Quantum Electron. 2 (3) (1996) 435–453.
[5] S. Yamashita, et al., Saturable absorbers incorporating carbon nanotubes directly synthesized onto substrates and fibers and their application to mode-locked fiber lasers, Opt. Lett. 29 (14) (2004) 1581–1583.
[6] D.-P. Zhou, et al., Tunable passively Q-switched erbium-doped fiber laser with carbon nanotubes as a saturable absorber, IEEE Photon. Technol. Lett. 22 (1) (2010) 9–11.
[7] B. Chen, et al., Q-switched fiber laser based on transition metal dichalcogenides MoS_2, MoS_2, WS_2, and WSe_2, Opt. Express 23 (20) (2015) 26723–26737.
[8] R. Woodward, et al., Wideband saturable absorption in few-layer molybdenum diselenide ($MoSe_2$) for Q-switching Yb-, Er-and Tm-doped fiber lasers, Optics Express 23 (15) (2015) 20051–20061.
[9] Z. Yu, et al., High-repetition-rate Q-switched fiber laser with high quality topological insulator Bi 2 Se 3 film, Opt. Express 22 (10) (2014) 11508–11515.
[10] J. Lee, et al., Passively Q-Switched 1.89-μm fiber laser using a bulk-structured Bi 2 Te 3 topological insulator, IEEE J. Sel. Top. Quantum Electron. 21 (1) (2015) 31–36.
[11] J. Sotor, et al., Mode-locked erbium-doped fiber laser based on evanescent field interaction with Sb_2Te_3 topological insulator, Appl. Phys. Lett. 104 (25) (2014) 251112.
[12] L. Kong, et al., Black phosphorus as broadband saturable absorber for pulsed lasers from 1 μm to 2.7 μm wavelength, Laser Phys. Lett. 13 (4) (2016) 045801.
[13] J. Sotor, et al., Black phosphorus saturable absorber for ultrashort pulse generation, Appl. Phys. Lett. 107 (5) (2015) 051108.
[14] Q. Bao, et al., Atomic-layer graphene as a saturable absorber for ultrafast pulsed lasers, Adv. Funct. Mater. 19 (19) (2009) 3077–3083.
[15] S. Lu, et al., Third order nonlinear optical property of Bi 2 Se 3, 2013, 21(2), p. 2072–2082.
[16] F. Bonaccorso, Z.J.O.M.E. Sun, Solution processing of graphene, topological insulators and other 2d crystals for ultrafast photonics. 2014. 4(1): p. 63-78.
[17] J.O. Island, et al., Environmental instability of few-layer black phosphorus, 2D Materials 2 (1) (2015) 011002.
[18] H. Ahmad, et al., C-band Q-switched fiber laser using titanium dioxide (TiO 2) as saturable absorber, IEEE Photon. J. 8 (1) (2015) 1–7.
[19] M. Rusdi, et al., Q-switched and mode-locked thulium doped fiber lasers with nickel oxide film saturable absorber, Opt. Commun. 447 (2019) 6–12.
[20] M. Rahman, et al., Holmium oxide film as a saturable absorber for 2 μm Q-switched fiber laser, Chin. Phys. Lett. 34 (5) (2017) 054201.
[21] E. Garmire, Resonant optical nonlinearities in semiconductors, IEEE J. Sel. Top. Quantum Electron. 6 (6) (2000) 1094–1110.
[22] Z. Zheng, et al., Microwave and optical saturable absorption in graphene, Opt. Express 20 (21) (2012) 23201–23214.
[23] B. Chen, et al., Q-switched fiber laser based on transition metal dichalcogenides MoS 2, MoSe 2, WS 2, and WSe 2, Opt. Express 23 (20) (2015) 26723–26737.
[24] M.F. Ab Rahman, et al., Ultrashort pulse soliton fiber laser generation with integration of antimony film saturable absorber, J. Lightwave Technol. 36 (16) (2018) 3522–3527.
[25] R. Wang, et al., Passively Q-switched and mode-locked fiber laser research based on graphene saturable absorbers, Opt. Quant. Electron. 49 (4) (2017) 137.
[26] C. Zhao, et al., Wavelength-tunable picosecond soliton fiber laser with topological insulator: Bi 2 Se 3 as a mode locker, Opt. Express 20 (25) (2012) 27888–27895.
[27] H. Liu, et al., Femtosecond pulse erbium-doped fiber laser by a few-layer MoS 2 saturable absorber, Opt. Lett. 39 (15) (2014) 4591–4594.
[28] Y. Chen, et al., Mechanically exfoliated black phosphorus as a new saturable absorber for both Q-switching and mode-locking laser operation, Opt. Express 23 (10) (2015) 12823–12833.
[29] Y. Xu, et al., Solvothermal synthesis and ultrafast photonics of black phosphorus quantum dots, Adv. Opt. Mater. 4 (8) (2016) 1223–1229.
[30] P. Yan, et al., Large-area tungsten disulfide for ultrafast photonics, Nanoscale 9 (5) (2017) 1871–1877.
[31] Y. Ge, et al., Broadband nonlinear photoresponse of 2D TiS2 for ultrashort pulse

generation and all-optical thresholding devices, Adv. Opt. Mater. 6 (4) (2018) 1701166.
[32] K. Zhang, et al., Q-switched and mode-locked Er-doped fiber laser using PtSe 2 as a saturable absorber, Photonics Res. 6 (9) (2018) 893–899.
[33] S. Salam, et al., FIrpic thin film as saturable absorber for passively Q-switched and mode-locked erbium-doped fiber laser, Opt. Fiber Technol. 50 (2019) 256–262.
[34] M. Baharom, et al., Lutetium (III) oxide film as passive mode locker device for erbium-doped fibre laser cavity, Opt. Commun. 446 (2019) 51–55.
[35] W.A. Khaleel, et al., Magnesium oxide (MgO) thin film as saturable absorber for passively mode locked erbium-doped fiber laser, Opt. Laser Technol. 115 (2019) 331–336.
[36] A. Nady, et al., Mode-locked erbium-doped fiber laser using vanadium oxide as saturable absorber, Chin. Phys. Lett. 35 (4) (2018) 044204.
[37] A. Nady, et al., Femtoseconds soliton mode-locked erbium-doped fiber laser based on nickel oxide nanoparticle saturable absorber, Chin. Optics Lett. 15 (10) (2017) 100602.